Parton structure of the photon beyond the leading order

M. Glück, E. Reya, and A. Vogt
Institut für Physik, Universität Dortmund, D-4600 Dortmund 50, Federal Republic of Germany
(Received 9 December 1991)

A consistent and technically efficient treatment of the photon structure functions at higher orders of perturbation theory is presented. A factorization scheme avoiding the common perturbative instability problems encountered in the large-x region is introduced. The resulting implications for a perturbative analysis of the photon structure in this recommended scheme are pointed out.

PACS number(s): 12.38.Bx, 13.65.+i, 14.80.Am

I. INTRODUCTION

Our present knowledge about the parton content of the photon is rather poor since $F_2^\gamma(x,Q^2)$, the only present source of information, is quite insensitive to the gluon distribution and involves only a linear combination of the photonic parton distributions. Forthcoming jet or direct-photon production experiments at high-energy e^+e^- or ep colliders will provide further independent information on $q^\gamma(x,Q^2)$ and $G^\gamma(x,Q^2)$ in particular also in the interesting low-x and/or high-Q^2 region. The theoretical analysis of these experiments will afford also calculations beyond the leading logarithmic order (LO) just as in the corresponding investigations of the nucleon partonic structure. Prior to this one needs, however, the tools for treating the parton Q^2 evolution in the next-to-leading logarithmic order [higher order (HO)]. Our paper is devoted to this issue. In particular we shall present the Mellin n-moment technique of solving the Q^2-evolution equations which proves to be very efficient for the nucleon in the low-x and/or high-Q^2 region since it avoids the many iterations involved in the more direct Bjorken-x space technique whose application to the photon should be performed along the lines presented in Refs. [1,2] or [3,4]. In addition, it is much easier to omit all inconsistent $O(\alpha_s)$ contributions to the photonic parton densities and to F_2^γ when using the analytic HO 2-loop solutions in n-moment space than working with the numerical solutions in Bjorken-x space obtained by iterations [2–4]. Furthermore, we suggest and analyze a new factorization scheme for HO calculations, where the direct-photon contribution to F_2^γ is absorbed into the photonic quark distributions. This allows for perturbative stability between LO and HO results and avoids the notorious negative pointlike HO contribution to $F_2^\gamma(x,Q^2)$ in the modified minimal subtraction ($\overline{\text{MS}}$) scheme for large values of x.

In Sec. II we present the appropriate evolution equations and their solutions in n-moment space while Sec. III is devoted to the important issue of factorization schemes and boundary conditions associated with these integrations. The analytic expressions needed for performing the Mellin inversions are finally presented in the Appendix which also includes various analytic expressions for HO splitting functions of the photon that are necessary if one chooses to solve the evolution equations directly in x space; transformations between different factorization schemes are also discussed, which might be relevant for future HO analyses of resolved photon contributions to leptonic and semihadronic processes.

II. PHOTONIC PARTON DISTRIBUTIONS AND THEIR EVOLUTIONS

Following as closely as possible the notation and methods presented in Ref. [1], the parton distributions $q^\gamma(x,Q^2)$ in the photon satisfy the well known inhomogeneous evolution equation

$$\frac{dq^\gamma(x,Q^2)}{d\ln Q^2}=k(x,Q^2)+P*q^\gamma\ , \tag{2.1}$$

where the $*$ product denotes the conventional convolution in Bjorken-x space

$$P*q^\gamma\equiv\int_x^1\frac{dy}{y}P(x/y,Q^2)q^\gamma(y,Q^2) \tag{2.2}$$

which reduces, in Mellin-n space, to a simple product $P^nq^{\gamma,n}$ with the nth moment being defined as

$$f^n(Q^2)\equiv\int_0^1 x^{n-1}f(x,Q^2)dx\ . \tag{2.3}$$

The photon-parton splitting functions $k(x,Q^2)$ and the purely hadronic splitting functions $P(x,Q^2)$ in Eq. (2.1) receive the following 1- and 2-loop contributions:

$$\begin{aligned}k&=\frac{\alpha}{2\pi}k^{(0)}(x)+\frac{\alpha\alpha_s(Q^2)}{(2\pi)^2}k^{(1)}(x)\ ,\\ P&=\frac{\alpha_s(Q^2)}{2\pi}P^{(0)}(x)+\left[\frac{\alpha_s(Q^2)}{2\pi}\right]^2P^{(1)}(x)\ ,\end{aligned} \tag{2.4}$$

where $\alpha\simeq\frac{1}{137}$ and

$$\frac{\alpha_s(Q^2)}{4\pi}\simeq\frac{1}{\beta_0\ln Q^2/\Lambda^2}-\frac{\beta_1}{\beta_0^3}\frac{\ln\ln Q^2/\Lambda^2}{(\ln Q^2/\Lambda^2)^2} \tag{2.5}$$

with $\beta_0=11-2f/3$, $\beta_1=102-38f/3$, and f being the number of active flavors. The evolution is straightfor-

ward for the flavor-nonsinglet case $q^\gamma \equiv q^\gamma_{\rm NS}$ where $k^{(i)}=k^{(i)}_{\rm NS}(x)$, $i=0,1$, can be found in Ref. [1] and $P^{(i)}=P^{(i)}_{\rm NS}(x)$ are given in Ref. [5] and/or [6]. In the flavor-singlet case, however, Eq. (2.1) becomes a (coupled) matrix equation with

$$\mathbf{q}^\gamma \equiv \begin{bmatrix} \Sigma^\gamma \\ G^\gamma \end{bmatrix}, \quad \hat{P}^{(i)} \equiv \begin{bmatrix} P^{(i)}_{qq} & P^{(i)}_{qg} \\ P^{(i)}_{gq} & P^{(i)}_{gg} \end{bmatrix}, \tag{2.6}$$

$$\mathbf{k}^{(0)} \equiv \begin{bmatrix} k^{(0)}_q \\ 0 \end{bmatrix}, \quad \mathbf{k}^{(1)} \equiv \begin{bmatrix} k^{(1)}_q \\ k^{(1)}_g \end{bmatrix},$$

where $\Sigma^\gamma \equiv \sum_f (q^\gamma + \bar{q}^\gamma)$. The hadronic splitting functions $P^{(1)}_{rr'}(x)$ can be found in Refs. [7] and [6], the $k^{(i)}_q(x)$ are specified in Ref. [1] and the photon-gluon splitting function is given by

$$k^{(1)}_g(x)=3f\langle e^2\rangle\frac{4}{3}\left[-16+8x+\frac{20}{3}x^2+\frac{4}{3x} -(6+10x)\ln x-2(1+x)\ln^2 x\right] \tag{2.7}$$

with $\langle e^k\rangle \equiv f^{-1}\sum_f e_q^k$ and where the $\delta(1-x)$ contribution, incorrectly included in Refs. [8,1] and in all subsequent publications, has been omitted. Such a diagonal term corresponds to the gluon self-energy contribution to the $C_F T_R$ term of $P^{(1)}_{gg}$, from where $k^{(1)}_g$ has been originally extracted, which obviously has to be dropped [9,10] for the off-diagonal photon-gluon splitting function $k^{(1)}_g$. We shall see, however, that the results derived with the correct expression (2.7) do not significantly deviate, except for G^γ in the large-x region, from the incorrect ones, obtained thus far, where the $-\delta(1-x)$ contribution to (2.7) has been erroneously used.

Solving the evolution equations (2.1) straightforwardly for $q^\gamma_{\rm NS}(x,Q^2)$ and $\mathbf{q}^\gamma(x,Q^2)$ by iteration, one encounters [1–4] higher-order terms in α_s which, in the relevant 2-loop order considered, amount to inconsistent contributions to the photon structure function $F_2^\gamma(x,Q^2)$; for example, when combined with the appropriate coefficient functions according to

$$\frac{1}{x}F_2^\gamma(x,Q^2)=q^\gamma_{\rm NS}(x,Q^2)+\langle e^2\rangle\Sigma^\gamma(x,Q^2) +\frac{\alpha_s(Q^2)}{4\pi}B_q * [q^\gamma_{\rm NS}+\langle e^2\rangle\Sigma^\gamma] +\langle e^2\rangle\frac{\alpha_s(Q^2)}{4\pi}B_G * G^\gamma +3f\langle e^4\rangle\frac{\alpha}{4\pi}B_\gamma(x) \tag{2.8}$$

with $q^\gamma_{\rm NS}\equiv\sum_f(e_q^2-\langle e^2\rangle)(q^\gamma+\bar{q}^\gamma)$ and the convolutions are defined in (2.2), while the $B_i(x)$ can be found in Ref. [1]. In order to avoid the spurious convention-dependent higher-order $O(\alpha_s)$ terms which arise from these convolutions [their complete inclusion affords a treatment of Eq. (2.1) beyond the order considered here], various rather cumbersome algorithms in x space have been suggested and employed [2–4] which allow one to separate the one-loop and the two-loop contributions to $q^\gamma_{\rm NS}(x,Q^2)$ and $\mathbf{q}^\gamma(x,Q^2)$. This separation then allows one to omit explicitly all spurious higher-order terms which appear in (2.8). It is, however, much easier to work directly in n-moment space where the solutions of Eq. (2.1) can be given analytically and thus the separation of the solutions into various powers of α_s is trivial. Furthermore this n-moment technique for the Q^2 evolution, together with its Mellin inversion to x space, proves to be very efficient in the low-x and/or high-Q^2 region, since it avoids the many numerical iterations involved in the more direct Bjorken-x space calculation. This situation is similar to the one encountered for nucleon structure functions [11,12].

Taking, according to Eq. (2.3), the nth moment of Eq. (2.1), the various convolutions simply factorize and the moments of the inhomogeneous LO and HO k terms in (2.4) are given by

$$k^{(i)n}_{\rm NS}=3f(\langle e^4\rangle-\langle e^2\rangle^2)\kappa^n_i,\quad k^{i(n)}_q=3f\langle e^2\rangle\kappa^n_i,$$
$$\kappa^n_0=2\frac{n^2+n+2}{n(n+1)(n+2)}, \tag{2.9}$$
$$\kappa^n_1=\frac{4}{3}\left[[S_1^2(n)-S_2(n)+\tfrac{5}{2}]\kappa^n_0-\frac{4}{n^2}S_1(n) +\frac{11n^4+26n^3+15n^2+8n+4}{n^3(n+1)^3(n+2)}\right],$$

with $S_l(n)\equiv\sum_{j=1}^n j^{-l}$ and

$$k^{(1)n}_g=3f\langle e^2\rangle\frac{4}{3}\left[-2\frac{2n^6+4n^5+n^4-10n^3-5n^2-4n-4}{(n-1)n^3(n+1)^3(n+2)}\right] \tag{2.10}$$

where the latter expression corresponds to the nth moment of Eq. (2.7); i.e., there is no additional constant term -1 inside the square brackets of (2.10) as previously incorrectly included [8] due to the absence of the $-\delta(1-x)$ term in Eq. (2.7). The moments of the 1- and 2-loop splitting functions are well known and can be found, for example, in Ref. [6]: $P^{(0)n}_{rr'}=-\gamma^{(0)n}_{rr'}/4$ with $\gamma^{(0)n}_{rr'}$ given by Eqs. (B14)–(B17), and $P^{(1)n}_{rr'}=-\gamma^{(1)n}_{rr'}/8$ with $\gamma^{(1)n}_{rr'}$ given

by Eqs. (B19)–(B22) of Ref. [6]; the same relations hold of course also for the NS splitting functions with $\gamma_{\rm NS}^{(0)}$ given by Eq. (B14) and [13] $\gamma_{\rm NS}^{(1)n}\equiv\gamma_{\rm NS}^{(1)n}(\eta=+1)$ given by Eq. (B18) of Ref. [6]. It is now straightforward to find the solution of Eq. (2.1) with the help of the evolution operator [14]

$$\left[1+\frac{\alpha_s(Q^2)}{2\pi}U\right]L^{-(2/\beta_0)P^{(0)n}}$$

with $L(Q^2)\equiv\alpha_s(Q^2)/\alpha_s(Q_0^2)$ and where U accounts for the 2-loop contributions. With this ansatz [14] one obtains

$$q^{\gamma,n}(Q^2)=q_{\rm PL}^{\gamma,n}(Q^2)+q_{\rm had}^{\gamma,n}(Q^2) \tag{2.11}$$

with the "pointlike" (inhomogeneous) HO solution given by

$$q_{\rm PL}^{\gamma,n}(Q^2)=\frac{4\pi}{\alpha_s(Q^2)}\left[1+\frac{\alpha_s(Q^2)}{2\pi}U\right][1-L^{1-(2/\beta_0)P^{(0)n}}]\frac{1}{1-\frac{2}{\beta_0}P^{(0)n}}\frac{\alpha}{2\pi\beta_0}k^{(0)n}$$
$$+[1-L^{-(2/\beta_0)P^{(0)n}}]\frac{1}{-P^{(0)n}}\frac{\alpha}{2\pi}\left[k^{(1)n}-\frac{\beta_1}{2\beta_0}k^{(0)n}-Uk^{(0)n}\right]+O(\alpha_s) \tag{2.12}$$

and the "hadronic" (homogeneous) HO solution

$$q_{\rm had}^{\gamma,n}(Q^2)=\left\{L^{-(2/\beta_0)P^{(0)n}}+\frac{\alpha_s(Q^2)}{2\pi}UL^{-(2/\beta_0)P^{(0)n}}-\frac{\alpha_s(Q_0^2)}{2\pi}L^{-(2/\beta_0)P^{(0)n}}U\right\}q_{\rm had}^{\gamma,n}(Q_0^2)$$
$$+O(\alpha_s^2)\ , \tag{2.13}$$

where care is taken everywhere about the *order* of terms since in the flavor-singlet case we have to deal with the matrices and vectors in (2.6). The LO results are of course entailed in these expressions by simply dropping all the obvious higher-order terms ($\beta_1, k^{(1)n}, U$) and therefore will not be written out separately.

In the flavor-singlet case the HO evolution matrix $U\equiv\hat{U}$ satisfies [14]

$$[\hat{U},\hat{P}^{(0)}]=\frac{\beta_0}{2}\hat{U}+\hat{R} \tag{2.14}$$

with $\hat{R}\equiv\hat{P}^{(1)n}-(\beta_1/2\beta_0)\hat{P}^{(0)n}$, which yields

$$\hat{U}=-\frac{2}{\beta_0}(\hat{P}_+\hat{R}\hat{P}_++\hat{P}_-\hat{R}\hat{P}_-)+\frac{\hat{P}_-\hat{R}\hat{P}_+}{\lambda_+^n-\lambda_-^n-\frac{1}{2}\beta_0}+\frac{\hat{P}_+\hat{R}\hat{P}_-}{\lambda_-^n-\lambda_+^n-\frac{1}{2}\beta_0} \tag{2.15}$$

with

$$\lambda_\pm^n=\tfrac{1}{2}[P_{qq}^{(0)n}+P_{gg}^{(0)n}\pm\sqrt{(P_{qq}^{(0)n}-P_{gg}^{(0)n})^2+4P_{qg}^{(0)n}P_{gq}^{(0)n}}]\ ,$$
$$\hat{P}_\pm\equiv\pm(\hat{P}^{(0)n}-\lambda_\mp^n 1)/(\lambda_+^n-\lambda_-^n)\ , \tag{2.16}$$
$$\hat{P}_\pm^2=\hat{P}_\pm,\quad \hat{P}_+\hat{P}_-=\hat{P}_-\hat{P}_+=0\ ,\quad \hat{P}_++\hat{P}_-=1\ .$$

Since $\hat{P}^{(0)n}=\lambda_+^n\hat{P}_++\lambda_-^n\hat{P}_-$, the remaining matrix expressions in Eq. (2.12) for $\mathbf{q}_{\rm PL}^{\gamma,n}$ and in Eq. (2.13) for $\mathbf{q}_{\rm had}^{\gamma,n}$ can be explicitly calculated using

$$f(\hat{P}^{(0)n})=f(\lambda_+^n)\hat{P}_++f(\lambda_-^n)\hat{P}_-\ . \tag{2.17}$$

For the flavor-nonsinglet case, the solutions (2.11)-(2.13) for $q_{\rm NS}^{\gamma,n}(Q^2)$ do not involve any matrices and Eq. (2.14) simply reduces to $U_{\rm NS}=-(2/\beta_0)R_{\rm NS}$.

With these explicit solutions at hand for the photonic parton distributions $q_{\rm NS}^{\gamma,n}$, $\Sigma^{\gamma,n}$, and $G^{\gamma,n}$ it is now straightforward to find the correct consistent combination with the Wilson coefficients according to Eq. (2.8) of the final expression for F_2^γ, for example, where spurious $O(\alpha_s,\alpha_s^2)$ terms should be omitted from the "pointlike" and hadronic contributions: Since $q_{\rm PL}^{\gamma,n}$ in (2.12) is of the general form

$$q_{\rm PL}^{\gamma,n}=\frac{4\pi}{\alpha_s}a^n+b^n+O(\alpha_s)\ , \tag{2.18}$$

this yields, when inserted into the nth moment of Eq. (2.8),

$$\int_0^1 x^{n-1}\frac{1}{x}F_{2,\rm PL}^\gamma(x,Q^2)dx$$
$$=\frac{4\pi}{\alpha_s}[a_{\rm NS}^n+\langle e^2\rangle a_\Sigma^n]+b_{\rm NS}^n+\langle e^2\rangle b_\Sigma^n$$
$$+B_q^n a_{\rm NS}^n+\langle e^2\rangle(B_q^n a_\Sigma^n+B_G^n a_G^n)$$
$$+3f\langle e^4\rangle\frac{\alpha}{4\pi}B_\gamma^n\ , \tag{2.19}$$

with [8,6]

$$B_q^n=\frac{4}{3}\left[\left(3-\frac{2}{n(n+1)}\right)S_1(n)+2S_1^2(n)-2S_2(n)+\frac{3}{n}+\frac{4}{n+1}+\frac{2}{n^2}-9\right],$$

$$B_G^n = 2f\left[\frac{1}{n^2}-\frac{1}{n}+\frac{6}{n+1}-\frac{6}{n+2}-\frac{n^2+n+2}{n(n+1)(n+2)}S_1(n)\right], \qquad (2.20)$$
$$B_\gamma^n = (2/f)B_G^n .$$

Again, the LO result for $F_{2,\mathrm{PL}}^\gamma$ is obtained from Eq. (2.19) by omitting all b^n and B^n terms. Although less important than for the pointlike terms, the hadronic contribution to F_2^γ may also be consistently constructed from (2.8) utilizing the hadronic distributions as given in (2.13).

For most experiments of present interest, all expressions above should correspond to the $f=3$ active light flavors u, d, and s. The contribution of the heavier quarks $h=c$, b, t to F_2^γ should, in the threshold region where $W \gtrsim 2m_h$ with $W^2 \equiv Q^2(1/x-1)$, be calculated according to the lowest-order (Bethe-Heitler) cross section $\gamma^*(Q^2)\gamma \to h\bar{h}$, similar to the case of deep-inelastic lepton-hadron scattering:

$$\frac{1}{x}F_{2,h}^\gamma(x,Q^2) = 3e_h^4\frac{\alpha}{\pi}\left\{\beta\left[8x(1-x)-1-x(1-x)\frac{4m_h^2}{Q^2}\right]+\left[x^2+(1-x)^2+x(1-3x)\frac{4m_h^2}{Q^2}-x^2\frac{8m_h^4}{Q^4}\right]\ln\frac{1+\beta}{1-\beta}\right\} \qquad (2.21)$$

with $\beta^2 = 1-4m_h^2x/(1-x)Q^2$. Far above the heavy-quark threshold region, $W \gg 2m_h$, the heavy-quark flavors are treated as the light (massless) u, d, s flavors: The inclusion of these heavy quarks h in the massless evolution equations is, as usual, assumed to follow the same pattern as for the light quarks [15], which implies, in the $\overline{\mathrm{MS}}$ scheme, the continuity of *all* the parton distributions as well as of $\alpha_s(Q^2)$ across the "threshold" $Q^2=m_h^2$. This yields the boundary condition $h^\gamma(x,m_h^2)=\bar{h}^\gamma(x,m_h^2)=0$ and a somewhat complicated expression [15] relating $\Lambda^{(f+1)}$ to $\Lambda^{(f)}$. Here $f+1$ denotes the number of the relevant active flavors at $Q^2 > m_h^2$ which should obviously be used in β_0 and β_1 as well as in all flavor factors appearing above. Note furthermore that the singlet combination Σ^γ in (2.6) now includes all the relevant active quarks with $m_q^2 \le Q^2$ and that the set of nonsinglet distributions $q_{\mathrm{NS}}^{\gamma,n}(Q^2)$ should be completed by all the relevant combinations, i.e., $(u^\gamma+\bar{u}^\gamma)+(d^\gamma+\bar{d}^\gamma)+(s^\gamma+\bar{s}^\gamma)-3(c^\gamma+\bar{c}^\gamma)$, $(u^\gamma+\bar{u}^\gamma)+(d^\gamma+\bar{d}^\gamma)+(s^\gamma+\bar{s}^\gamma)+(c^\gamma+\bar{c}^\gamma)-4(b^\gamma+\bar{b}^\gamma)$, etc.

All the above solutions in moment-n space may be converted into the desired x-space expressions by utilizing the Mellin inversion of Eq. (2.3): i.e.,

$$f(x,Q^2) = \frac{1}{\pi}\int_0^\infty dz\ \mathrm{Im}[e^{i\varphi}x^{-c-ze^{i\varphi}}f^{n=c+ze^{i\varphi}}(Q^2)] , \qquad (2.22)$$

where the contour of integration, and thus the value of c, has to lie to the right of all singularities of $f^n(Q^2)$ in the complex n plane. For all practical purposes one may choose [12] $\varphi = 135°$ and $c=0.8$ for the nonsinglet and $c=1.8$ for the singlet sector inversions. The upper limit of integration in (2.22) may be taken to be $5+10/\ln x^{-1}$, as can be estimated from (2.22) with a slowly varying f^n for $n \gg 1$, which suffices to guarantee accurate and stable numerical results for all nonsinglet and singlet inversions considered. The Mellin inversion (2.22) affords the analytic continuation in n of the moments f^n. The only obstacle lies in the higher-order $\gamma_{\mathrm{NS}}^{(1),n}$ and $\gamma_{rr'}^{(1),n}$ which were originally presented [6] only for integer values of n. The prescriptions for the relevant analytic continuations [12] are, for completeness, recapitulated in the Appendix.

III. FACTORIZATION SCHEMES AND BOUNDARY CONDITIONS FOR HO PHOTONIC PARTON DISTRIBUTIONS

The (regular) solutions in (2.11) of the evolution equations depend on the unspecified hadronic input distributions at $Q^2=Q_0^2$ which, as in the case of the nucleon, can either be determined by a multitude of dedicated experiments, i.e., phenomenologically, or via some reasonable physical assumptions, e.g., the ones proposed in Refs. [12,16,17]. Up to now the phenomenological investigations were restricted to $F_2^\gamma(x,Q^2)$, which does not suffice for delineating the various parton distributions since it depends only on their linear combination according to Eq. (2.8) or (2.19). The first two terms in (2.8) represent the LO contribution to F_2^γ and the remaining HO terms refer to the $\overline{\mathrm{MS}}$ factorization scheme which, so far, has been used to define and calculate HO parton distributions, splitting functions and coefficient functions [8,6,14]. In this $\overline{\mathrm{MS}}$ scheme one notes that the last B_γ term in (2.8), which is negative and diverges in the large-x region, $B_\gamma(x) \simeq 4[\ln(1-x)-1]$, could drive $F_2^\gamma(x,Q^2)$ to physically unacceptable negative values [2] as $x \to 1$ if in HO one takes over "naively" the LO boundary conditions for the photonic parton distributions at $Q^2=Q_0^2$. This is illustrated in Fig. 1 for the pointlike solution in Eq. (2.12). Clearly the addition of the conventional hadronic contribution in (2.13), where the input $q_{\mathrm{had}}^\gamma(x,Q_0^2)$ is usually related to the pionic distributions via vector-meson dominance (VMD) [18,2], will slightly improve the situation; but even with a fine-tuning of the hadronic input parameters, the VMD input alone, which vanishes as $x \to 1$, is not sufficient to avoid negative values of $F_2^\gamma(x,Q^2)$ throughout the whole x region and for all $Q^2 \ge Q_0^2$ [2,4]. Furthermore, one notes from Fig. 1 that the pointlike HO $\overline{\mathrm{MS}}_{\mathrm{naive}}$ predictions, given in (2.12), differ drastically from the LO ones. This requires the hadronic HO input in (2.13) to be appropriately adjusted

and substantially different from the LO one, in order to partly avoid sizeable perturbative instabilities for the full LO and HO solution (2.11), in particular for $F_2^\gamma(x,Q^2)$.

In order to circumvent such inconsistencies in HO ($\overline{\text{MS}}$) calculations, which are mainly caused by the B_γ term in Eq. (2.8) or (2.19), it seems to be more appropriate to change the pointlike HO boundary conditions at $Q^2=Q_0^2$ in order to compensate the troublesome B_γ contribution or, equivalently, to search for a different factorization scheme which does not have the problems of the $\overline{\text{MS}}$ scheme naively implemented as discussed above and allows for the same pointlike input as in LO. Such a factorization scheme can be easily found by removing the B_γ term in (2.8) from F_2^γ and absorbing it into the quark distributions. This redefinition of the photonic distributions implies, of course, also a transformation of the photonic HO splitting functions $k^{(1)}$ in (2.4) which can be most easily derived from the nonsinglet and singlet evolution equations for F_2^γ in the moment n space: The transformation $B_\gamma^n \to B_\gamma^n + \delta B_\gamma^n = 0$, i.e., $\delta B_\gamma^n = -B_\gamma^n$ implies for the $k^{(1)n}$ in Eqs. (2.9) and (2.10) the transformations $k^{(1)n} \to k^{(1)n} + \delta k^{(1)n}$ with

$$\delta k_{\text{NS}}^{(1)n} = -3f(\langle e^4\rangle - \langle e^2\rangle^2)\tfrac{1}{2}P_{qq}^{(0)n}B_\gamma^n \ ,$$
$$\delta \mathbf{k}^{(1)n} = \begin{pmatrix} \delta k_q^{(1)n} \\ \delta k_g^{(1)n} \end{pmatrix} = 3f\langle e^2\rangle \frac{1}{2} \begin{pmatrix} P_{qq}^{(0)n}B_\gamma^n \\ P_{gq}^{(0)n}B_\gamma^n \end{pmatrix} . \tag{3.1}$$

We shall call this factorization scheme DIS_γ since only the purely photonic higher order B_γ term has been, by definition, transformed into the photonic quark distributions in contrast with the full DIS (deep-inelastic scattering) scheme [11,19] where *all* the HO contributions to F_2, i.e., also the B_q and B_g terms, are absorbed into the quark distributions. The advantage of the DIS_γ scheme is that we can use the *same* boundary conditions for the pointlike LO *and* HO distributions,

$$q_{\text{PL}}^\gamma(x,Q_0^2) = \bar{q}_{\text{PL}}^\gamma(x,Q_0^2) = G_{\text{PL}}^\gamma(x,Q_0^2) = 0 \ , \tag{3.2}$$

without violating the usual positivity requirements. It should be noted that the evolution of $q_{\text{had}}^{\gamma,n}(Q^2)$ in (2.13) is unaffected by the transformation (3.1) and, most importantly, that in DIS_γ the experimental inputs $q_{\text{had}}^\gamma(x,Q_0^2)$ in LO and HO differ just by the usual *small* amounts encountered, e.g., in the study of the nucleon or pion structure.

The advantage of the DIS_γ factorization scheme is not restricted to F_2^γ alone but extends also to other physical processes plagued by an identical HO negative, $\ln(1-x)$, unresolved photon contribution. For example, $d\sigma(\gamma p \to VX)/dx_F$ with $V=\gamma^*,W,Z$ is dominated by a HO negative $\ln(1-x_F)$ contribution induced by the unresolved photon subprocess $\gamma q \to Vq'$ which is of HO in α_s as compared to the LO resolved photon subprocess $\bar{q}'^\gamma q \to V$.

In Figs. 1–3 we present the pointlike solutions (2.12) for $F_{2,\text{PL}}^\gamma$, $\Sigma_{\text{PL}}^\gamma$, and G_{PL}^γ, obtained for $Q_0^2=1$ GeV^2, $\Lambda_{\text{LO}}=\Lambda_{\text{HO}}=200$ MeV and for $f=3$ flavors using the same boundary conditions (3.2) in LO and HO ($\overline{\text{MS}}_{\text{naive}}$ and DIS_γ). It should be clear by now that $\overline{\text{MS}}_{\text{naive}}$ obviously refers to the physically inferior straightforward solutions (2.12) in the $\overline{\text{MS}}$ scheme used thus far, in contrast to the DIS_γ solutions where the $k^{(1)n}$ in (2.9) and (2.10) are replaced according to (3.1). Comparing the HO results for the DIS_γ and the $\overline{\text{MS}}_{\text{naive}}$ scheme with the LO solutions, it becomes obvious that perturbative stability

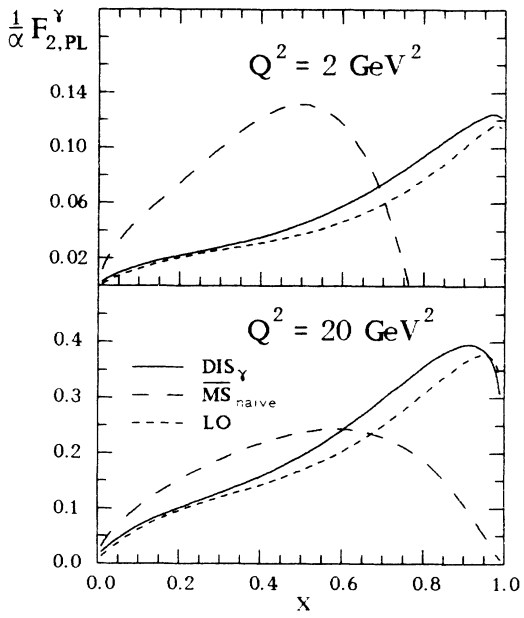

FIG. 1. The pointlike LO and HO solutions for F_2^γ in the $\overline{\text{MS}}_{\text{naive}}$ and DIS_γ schemes resulting from Eq. (2.12) which corresponds to the vanishing input (3.2), using $Q_0^2=1$ GeV^2, $\Lambda_{\text{LO}}=\Lambda_{\text{HO}}=0.2$ GeV, and $f=3$. The results for the DIS_γ scheme are obtained from Eq. (2.19) with $B_\gamma^n \equiv 0$ using the solutions in Eq. (2.12) with $k^{(1)}$ transformed according to (3.1).

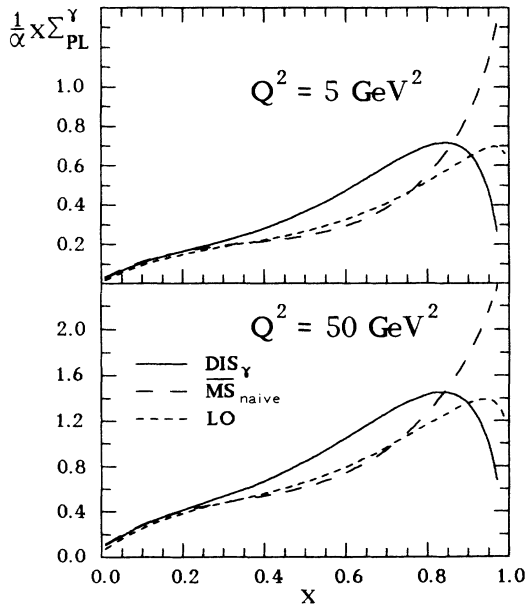

FIG. 2. The pointlike LO and HO flavor-singlet solutions $\Sigma^\gamma(x,Q^2)$ resulting from Eq. (2.12). The notations and parameters are as in Fig. 1.

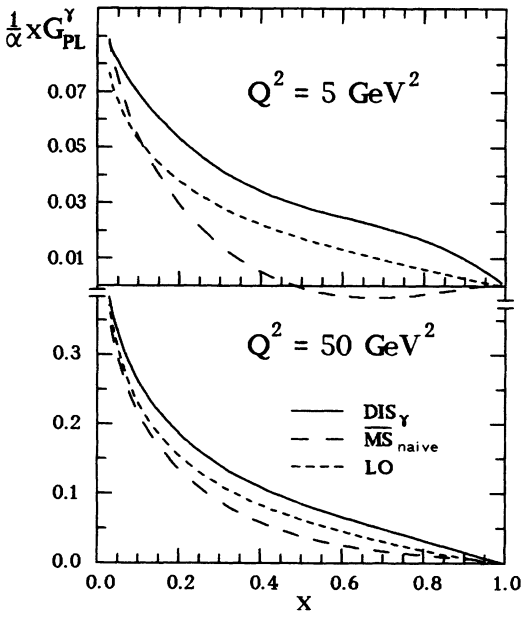

FIG. 3. The pointlike LO and HO solutions for the photonic gluon distribution $G^{\gamma}(x,Q^2)$ resulting from Eq. (2.12). The notation and parameters are as in Fig. 1.

for $F_2^{\gamma}(x,Q^2)$ throughout the entire x region can only be achieved in DIS_{γ} where, moreover, the distributions are manifestly positive [20] for all $Q^2 \geq Q_0^2$, in contrast with the $\overline{MS}_{naive}$ scheme. As illustrated in Fig. 3, $G^{\gamma}_{PL}(x,Q^2)$ turns negative in the larger x region in the $\overline{MS}_{naive}$ scheme for Q^2 not much larger than Q_0^2, in contrast with DIS_{γ}. It should furthermore be noted that our $\overline{MS}_{naive}$ results for $x\Sigma^{\gamma}_{PL}(x,Q^2)$ and $xG^{\gamma}_{PL}(x,Q^2)$ in Figs. 2 and 3 for $Q^2=50\ GeV^2$ differ from those of Ref. [10], in particular for G^{γ}_{PL} where our result is up to a factor of 2.5 smaller for $x \gtrsim 0.5$.

The $x \to 0$ behavior of the "asymptotic" solution [8,1–3] $F^{\gamma,n}_{2,asy}(Q^2)$, to be derived from Eqs. (2.11)–(2.13) for $L \to 0$, i.e., $\alpha_s(Q^2) \to 0$, can be given analytically in the following way: Inserting these asymptotic solutions into Eq. (2.19) one notes that, for $x \to 0$, the dominant contribution derives from b^n_{Σ} due to its well-known pole at $n=2$:

$$\left[\frac{1}{x}F^{\gamma}_{2,asy}\right]^n \simeq \langle e^2\rangle b^n_{\Sigma,asy} = \alpha\frac{R}{n-2} + \bar{b}^{\,n} \tag{3.3}$$

with $\bar{b}^{\,n}$ being regular at $n=2$ and

$$R = \langle e^2\rangle \frac{2}{\pi}\left[-4\frac{d\lambda^n_-}{dn}\right]^{-1}_{n=2}(\hat{P}_-)^{n=2}_{qq} \times \left[-\frac{\beta_1}{2\beta_0}k_q^{(0)2} + k_q^{(1)2} + k_g^{(1)2}\right]$$

which, for $f=4$, yields $R=-0.007\,72$ as compared to $R=-0.0220$ for the incorrect $k_g^{(1)n}$ of Ref. [8], as discussed after Eq. (2.10). This drastic change of the $n=2$ residue is due to the fact that $k_q^{(1)2}+k_g^{(1)2}>0$ according to Eqs. (2.9) and (2.10), whereas $k_q^{(1)2}+k_g^{(1)2}=0$ for the incorrect $k_g^{(1)n}$ of Ref. [8]. Thus the notorious negative spike [21] of the HO asymptotic solution in the small-x region,

$$\frac{1}{x}F^{\gamma}_{2,asy}(x,Q^2) \sim \alpha R x^{-2},$$

is diminished drastically and affects only the very small x region. This obviously modifies the regularization terms proposed in Ref. [22]. The full pointlike solution in (2.12) is, on the other hand, of course regular [1,2] and (small-x) singularities such as the one in (3.3) as well as their relative size become immaterial [20].

Our results suggest that it is recommendable to work with photonic parton distributions in the DIS_{γ} scheme, obtained via the transformation (3.1), if one attempts to study the importance of the resolved photon components beyond the LO in leptonic or semihadronic hard processes. Since most of the required HO partonic subprocesses have been calculated in the $\overline{MS}$ scheme [23,24], one has of course to transform some of these subprocesses into the DIS_{γ} scheme in order to perform a consistent theoretical analysis. Alternatively one could, of course, transform just the DIS_{γ} distributions into their $\overline{MS}$ counterparts compatible with the published HO ($\overline{MS}$) subprocess cross sections. Since, furthermore, no full HO analysis has been performed so far using the HO photonic quark and gluon distributions, we discuss in the Appendix the transformations between different factorization schemes for the typical example of deep-inelastic ep scattering where details of the resolved photon structure can be studied most directly.

IV. SUMMARY AND CONCLUSIONS

We have presented in detail all expressions pertaining to a technically efficient and theoretically consistent treatment of the photon structure functions in higher-order (HO) perturbative QCD. The special DIS_{γ} factorization scheme, introduced in Sec. III, was shown to evade the appearance of undesired instabilities, in particular in the large-x region, usually encountered in HO calculations performed within the framework of the $\overline{MS}$ scheme as caused by the "naively" chosen boundary conditions for the pointlike solution (i.e., vanishing HO input at $Q^2=Q_0^2$ as in the LO case) of the renormalization-group evolution equations. This choice, motivated by the desire to keep the hadronlike solution of the Q^2 evolution equations as stable as possible, was shown to be realizable only within the framework of the aforementioend DIS_{γ} scheme.

The advantage of the DIS_{γ} factorization scheme is real in the sense that only within this framework do the hadronic input distributions retain their physically expected x shapes also in higher orders of perturbative QCD. Thus the extraction of these, *a priori* unknown, input distributions from the experimental data is assured to be as straightforward as in the corresponding nucleon or pion case when working in higher orders of perturbative QCD,

provided one operates within the framework of the recommended DIS_γ factorization scheme.

ACKNOWLEDGMENTS

This work was supported in part by the "Bundesministerium für Forschung und Technologie," Bonn.

APPENDIX

Inverting anomalous dimensions and Wilson coefficients

The appropriate n moments of 1- and 2-loop anomalous dimensions in Eq. (2.6) are summarized in Eqs. (B.14)–(B.22) in Appendix B of Ref. [6]. The color factors are $C_A=3$ and $C_F=\frac{4}{3}$. According to our approach, explained in Sec. II, one should use in $T_R=f/2$ the appropriate number of active flavors in the Q^2 range considered. The analytic continuations in n, required by the Mellin inversion (2.22), are straightforward, except for the following nontrivial sums which are to be continued in the following way [25]:

$$S_1(n)\equiv\sum_{j=1}^{n}\frac{1}{j}=\gamma_E+\psi(n+1),\quad \gamma_E=0.577\,216\ , \tag{A1}$$

$$S_2(n)\equiv\sum_{j=1}^{n}\frac{1}{j^2}=\zeta(2)-\psi'(n+1),\quad \zeta(2)=\pi^2/6\ , \tag{A2}$$

$$S_3(n)\equiv\sum_{j=1}^{n}\frac{1}{j^3}=\zeta(3)+\tfrac{1}{2}\psi''(n+1),\quad \zeta(3)=1.202\,057\ , \tag{A3}$$

where $\psi^{(k)}(z)=d^{(k+1)}\ln\Gamma(z)/dz^{k+1}$ can be sufficiently accurately expressed by asymptotic sums to be given below; furthermore

$$S_l'(\tfrac{1}{2}n)\equiv 2^{l-1}\sum_{j=1}^{n}\frac{1+(-)^j}{j^l}=\tfrac{1}{2}(1+\eta)S_l\left[\frac{n}{2}\right]+\tfrac{1}{2}(1-\eta)S_l\left[\frac{n-1}{2}\right] \tag{A4}$$

$$\tilde{S}(n)\equiv\sum_{j=1}^{n}\frac{(-)^j}{j^2}S_1(j)=-\frac{5}{8}\zeta(3)+\eta\left[\frac{S_1(n)}{n^2}-\frac{\zeta(2)}{2}G(n)+\int_0^1 dx\,x^{n-1}\frac{\mathrm{Li}_2(x)}{1+x}\right] \tag{A5}$$

with $G(n)\equiv\psi((n+1)/2)-\psi(n/2)$, $\mathrm{Li}_2(x)=-\int_0^x z^{-1}\ln(1-z)dz$, and where [5] $\eta\equiv(-)^n\to+1$ for our photonic nonsinglet [13] as well as singlet distributions. Since the integral in (A5), involving the dilogarithm Li_2, cannot be reduced to a known analytic function anymore, we have parametrized the integrand by the simple, sufficiently accurate expression

$$\frac{\mathrm{Li}_2(x)}{1+x}\simeq 1.010x-0.846x^2+1.155x^3-1.074x^4+0.550x^5 \tag{A6}$$

which allows for an elementary calculation of the required moment integral in (A5). The various ψ functions and their derivatives appearing in the above expressions were calculated, for $\mathrm{Re}z\geq 10$, with the help of the asymptotic expansions [25]

$$\psi(z)\simeq\ln z-\frac{1}{2z}-\frac{1}{12z^2}+\frac{1}{120z^4}-\frac{1}{252z^6}\ , \tag{A7}$$

$$\psi'(z)\simeq\frac{1}{z}+\frac{1}{2z^2}+\frac{1}{6z^3}-\frac{1}{30z^5}+\frac{1}{42z^7}-\frac{1}{30z^9}\ , \tag{A8}$$

$$\psi''(z)\simeq-\frac{1}{z^2}-\frac{1}{z^3}-\frac{1}{2z^4}+\frac{1}{6z^6}-\frac{1}{6z^8}+\frac{3}{10z^{10}}-\frac{5}{6z^{12}}\ . \tag{A9}$$

For $\mathrm{Re}z<10$ we have repeatedly used the recursion relation

$$\psi^{(k)}(z+1)=\psi^{(k)}(z)+(-)^k k!\,z^{-k-1} \tag{A10}$$

in order to reach $\psi^{(k)}(z)$ with $\mathrm{Re}z\geq 10$. The derivation of Eq. (A5) can be found in Ref. [12].

Mellin inversions of photonic HO splitting functions

With the analytic continuations in n discussed above in the first part of this appendix, the (numerical) Mellin inversions of the additional contributions to the HO splitting functions of the photon in Eq. (3.1), needed for obtaining the photonic parton distributions in the DIS_γ scheme, are straightforward. If one chooses, however, to solve the evolution equations (2.1) by (numerical) iteration in x space for the DIS_γ photonic parton distributions, the Mellin inverse of $\delta k_i^{(1)n}$ in Eq. (3.1) is explicitly needed. The two products of moments in (3.1) between

$$P_{qq}^{(0)n}=C_F\left[\frac{3}{2}+\frac{1}{n}-\frac{1}{n+1}-2S_1(n)\right],$$

$$P_{gq}^{(0)n}=C_F\left[\frac{2}{n-1}-\frac{2}{n}+\frac{1}{n+1}\right]$$

and B_γ^n in Eq. (2.20) can be analytically inverted using standard Mellin-moment integrals [26]. For $\kappa_q^n\equiv P_{qq}^{(0)n}B_\gamma^n$ we obtain

$$\kappa_q(x)=2C_F\left\{7-10x-\frac{\pi^2}{6}(6-12x+16x^2)+(1-16x+32x^2)\ln x\right.$$
$$+(1-2x+4x^2)\ln^2 x-(5-36x+32x^2)\ln(1-x)$$
$$\left.+(4-8x+8x^2)[\ln^2(1-x)-\ln x\ln(1-x)]+(2-4x+8x^2)\mathrm{Li}_2(x)\right\} \quad \text{(A11)}$$

and the inverse of $\kappa_g^n \equiv P_{gq}^{(0)n} B_\gamma^n$ turns out to be

$$\kappa_g(x)=4C_F\left\{\frac{2}{3x}-\frac{20}{3}+\frac{2}{3}x+\frac{16}{3}x^2\right.$$
$$-(1+5x-\tfrac{4}{3}x^2)\ln x-(1+x)\ln^2 x$$
$$+\left[\frac{4}{3x}+1-x-\frac{4}{3}x^2\right]\ln(1-x)$$
$$\left.-2(1+x)[\mathrm{Li}_2(x)-\pi^2/6]\right\}. \quad \text{(A12)}$$

A helpful nonstandard formula required for obtaining (A11) is given by

$$\int_0^1 dx\, x^{n-1}x^a[\ln^2(1-x)-\ln x\ln(1-x)-\mathrm{Li}_2(x)]$$
$$=\frac{1}{n+a}[S_1(n+a)]^2 .$$

These results agree with a previous calculation involving the gluonic coefficient function [27].

Transformations between different factorization schemes

In order to elucidate the transformation between different factorization schemes let us, for definiteness, consider the realistic example of deep-inelastic *ep* scattering which so far has been studied only in LO as a test of photonic parton distributions at the DESY *ep* collider HERA [28]. Generically the (virtual) photon-proton cross section is of the form

$$\sigma^{\gamma p}=\sum_f f*\hat{\sigma}^{\gamma f}+\sum_{f^\gamma}\sum_f f^\gamma * f*\hat{\sigma}^{f^\gamma f} \quad \text{(A13)}$$

with f and f^γ denoting the partons within the proton and the photon, respectively. The direct photon-parton subprocesses are denoted by $\hat{\sigma}^{\gamma f}$ and the purely hadronic subprocesses by $\hat{\sigma}^{f^\gamma f}$ which we assume to have been calculated in HO in the $\overline{\mathrm{MS}}$ scheme as is commonly the case [23]. Therefore, f^γ in (A13) has to refer to the $\overline{\mathrm{MS}}$ scheme as well, to be obtained from the transformation

$$f^\gamma_{\overline{\mathrm{MS}}}=f^\gamma_{\mathrm{DIS}_\gamma}+\delta f^\gamma \quad \text{(A14)}$$

with

$$\delta q^\gamma=\delta\bar{q}^\gamma=-3e_q^2\frac{\alpha}{8\pi}B_\gamma\ ,\quad \delta G^\gamma=0 \quad \text{(A15)}$$

which simply follows from the requirement than in DIS_γ the B_γ term in Eq. (2.8) or (2.19) has, by definition, to be absorbed into the photonic quark distributions. Note that the transformed $\overline{\mathrm{MS}}$ quark and antiquark distributions in Eq. (A14) differ [29] from the conventional $\overline{\mathrm{MS}}_{\mathrm{naive}}$ ones discussed in Sec. III due to their *nonvanishing* boundary conditions at $Q^2=Q_0^2$.

Alternatively, if one continues to work directly with $f^\gamma_{\mathrm{DIS}_\gamma}$ one has to use, in order to keep $\sigma^{\gamma p}$ invariant, in (A13) the transformation

$$\hat{\sigma}^{\gamma f}_{\mathrm{DIS}_\gamma}=\hat{\sigma}^{\gamma f}+\sum_{f^\gamma}\delta f^\gamma * \hat{\sigma}^{f^\gamma f} \quad \text{(A16)}$$

with δf^γ given by (A15). Note that the purely hadronic quantities $(f,\hat{\sigma}^{f^\gamma f})$ remain unchanged.

[1] M. Glück and E. Reya, Phys. Rev. D **28**, 2749 (1983).
[2] M. Glück, K. Grassie, and E. Reya, Phys. Rev. D **30**, 1447 (1984).
[3] G. Rossi, Phys. Lett. **130B**, 105 (1983); Phys. Rev. D **29**, 852 (1984); M. Drees, Z. Phys. C **27**, 123 (1985).
[4] J. H. Da Luz Vieira and J. K. Storrow, Phys. Lett. B **205**, 367 (1988); **219**, 529(E) (1989); Z. Phys. C **51**, 241 (1991).
[5] G. Curci, W. Furmanski, and R. Petronzio, Nucl. Phys. **B175**, 27 (1980).
[6] E. G. Floratos, C. Kounnas, and R. Lacaze, Nucl. Phys. **B192**, 417 (1981).
[7] W. Furmanski and R. Petronzio, Phys. Lett. **97B**, 437 (1980).
[8] W. A. Bardeen and A. J. Buras, Phys. Rev. D **20**, 166 (1979); **21**, 2041(E) (1980).
[9] This has been noted independently also in Ref. [10].
[10] M. Fontannaz and E. Pilon, Phys. Rev. D **45**, 382 (1992).
[11] M. Diemoz, F. Ferroni, E. Longo, and G. Martinelli, Z. Phys. C **39**, 21 (1988).
[12] M. Glück, E. Reya, and A. Vogt, Z. Phys. C **48**, 471 (1990).
[13] It should be noted that, in contrast with the nucleon case, q^γ_{NS} always evolves with $P^{(0)}_{\mathrm{NS}}(x)=P^{(0)}_{qq}(x)$ and $P^{(1)}_{\mathrm{NS}}(x)\equiv P^{(1)}_{\mathrm{NS},+}(x)$ in the notation of Refs. [5,6] or in moment space with $P^{(0)n}_{\mathrm{NS}}=-\gamma^{(0)n}_{\mathrm{NS}}/4$ and $P^{(1)n}_{\mathrm{NS}}=-\gamma^{(1)n}_{\mathrm{NS}}/8$ with $\gamma^{(1)n}_{\mathrm{NS}}\equiv\gamma^{(1)n}_{\mathrm{NS}}(\eta=+1)$ given by Eq. (B.18) of Ref. [6]. This is so, because the nonsinglet combination for $\eta=-1$ corresponds to $u^\gamma-\bar{u}^\gamma$ and $d^\gamma-\bar{d}^\gamma$ which vanish identi-

cally, while the one for $\eta=+1$ corresponds to the non-singlet combinations $(u^\gamma+\bar{u}^\gamma)-(d^\gamma+\bar{d}^\gamma)$, $(u^\gamma+\bar{u}^\gamma)+(d^\gamma+\bar{d}^\gamma)-2(s^\gamma+\bar{s}^\gamma)$, etc.

[14] W. Furmanski and R. Petronzio, Z. Phys. C **11**, 293 (1982).

[15] J. C. Collins and W. K. Tung, Nucl. Phys. **B278**, 934 (1986).

[16] M. Glück, E. Reya, and A. Vogt, Z. Phys. C **53**, 127 (1992).

[17] M. Glück and E. Reya, Nucl. Phys. **B311**, 519 (1988/89).

[18] Ch. Berger and W. Wagner, Phys. Rep. **146**, 1 (1987).

[19] G. Altarelli, R. K. Ellis, and G. Martinelli, Nucl. Phys. **B143**, 521 (1978); **B146**, 544(E) (1978).

[20] If the incorrect $k_g^{(1)n}$ of Ref. [8] were used, as discussed after Eq. (2.10), then the HO gluon distributions, shown in Fig. 3 would not remain positive in the large-x region, in either the $\overline{\text{MS}}_{\text{naive}}$ or in the DIS_γ scheme: In the latter scheme, for example, xG_{PL}^γ would become negative for $x \gtrsim 0.8$, whereas in the $\overline{\text{MS}}_{\text{naive}}$ scheme xG_{PL}^γ turns negative already at smaller values of x depending on Q^2 (e.g., $x \simeq 0.4$ for $Q^2=5$ GeV^2). The changes in the small-x region ($x \lesssim 0.1$) are, however, immaterial (less than 20%) as compared to the results corresponding to the correct $k_g^{(1)n}$ in Eq. (2.10).

[21] D. W. Duke and J. F. Owens, Phys. Rev. D **22**, 2280 (1980).

[22] I. Antoniadis and G. Grunberg, Nucl. Phys. **B213**, 445 (1983); I. Antoniadis and L. Marleau, Phys. Lett. **161B**, 163 (1985).

[23] R. K. Ellis, M. A. Furman, H. E. Haber, and I. Hinchliffe, Nucl. Phys. **B173**, 397 (1980); R. K. Ellis and J. C. Sexton, *ibid.* **B269**, 445 (1986); F. Aversa, P. Chiappetta, M. Greco, and J. Ph. Guillet, Phys. Lett. B **210**, 225 (1988); **211**, 465 (1988); Nucl. Phys. **B327**, 105 (1989); Z. Phys. C **46**, 253 (1990); P. Nason, S. Dawson, and R. K. Ellis, Nucl. Phys. **B303**, 607 (1988); **B327**, 49 (1989); W. Beenacker, H. Kuijf, W. L. van Neerven, and J. Smith, Phys. Rev. D **40**, 54 (1989); W. Beenacker, W. L. van Neerven, R. Meng, G. A. Schuler, and J. Smith, Nucl. Phys. **B351**, 507 (1991).

[24] R. K. Ellis and P. Nason, Nucl. Phys. **B312**, 551 (1989); D. W. Duke and J. F. Owens, Phys. Rev. D **26**, 1600 (1982); **28**, 1227(E) (1983); P. Aurenche, A. Douiri, R. Baier, M. Fontannaz, and D. Schiff, Z. Phys. C **24**, 309 (1984).

[25] M. Abramowitz and I. A. Stegun, *Handbook of Mathematical Functions* (Dover, New York, 1968).

[26] A useful collection can be found in A. Devoto and D. W. Duke, Florida State University Report No. FSU-HEP-831003, 1983 (unpublished).

[27] R. T. Herrod, S. Wada, and B. R. Webber, Z. Phys. C **9**, 351 (1981).

[28] M. Drees and R. M. Godbole, Phys. Rev. Lett. **61**, 682 (1988); **67**, 1189 (1991); Phys. Rev. D **39**, 169 (1989); Nucl. Phys. **B339**, 355 (1990).

[29] Because of Eqs. (A14) and (A15), i.e., $q^\gamma(x,Q_0^2)_{\overline{\text{MS}}} \sim -B_\gamma(x)$, the transformed $\overline{\text{MS}}$ photonic quark distributions increase even faster in the large-x region than their $\overline{\text{MS}}_{\text{naive}}$ counterparts shown in Fig. 2. For the same reason, these pointlike transformed $\overline{\text{MS}}$ densities become sometimes negative (in the small- and medium-x region depending on the value of Q^2 not much larger than Q_0^2), but the total photonic quark distributions in Eq. (2.11), with the hadronic piece added, remain of course positive. Furthermore, beause of the strong increase of $\sum_{\overline{\text{MS}}}^\gamma(x,Q^2)$ in the large-x region, cf. Fig. 2, one might superficially conclude that HO calculations become perturbatively unstable as compared to LO results, which involve the far flatter LO distributions as $x \to 1$ in Fig. 2. An explicit HO analysis of deep-inelastic heavy-quark production has revealed that, after performing the relevant convolutions in Eq. (A13) using the relevant hadronic HO subprocesses of Ref. [23], this is not the case and that moreover the results are rather insensitive to the behavior of photonic parton distributions in the large-x region [M. Glück, E. Reya, and A. Vogt, Phys. Lett. B (to be published)].